Available online at www.CivileJournal.org

Civil Engineering Journal

(E-ISSN: 2476-3055; ISSN: 2676-6957)

Vol. 10, No. 10, October, 2024

Performance of Treated Date Palm Leaf Fiber as a Sustainable Reinforcement for Different Soil

Noor S. Al-Hassnawi [1, 2], Mastura Azmi [1*], Mohammed Y. Fattah [3], Fauziah Ahmad [1]

[1] *School of Civil Engineering, Universiti Sains Malaysia, 14300 Nibong Tebal, Malaysia.*

[2] *Roads and Transportation Engineering Department, College of Engineering, University of Al-Qadisiyah, Al-Qadisiyah, Iraq.*

[3] *Department of Civil Engineering, University of Technology, Baghdad, Iraq.*

Received 15 June 2024; Revised 09 September 2024; Accepted 16 September 2024; Published 01 October 2024

Abstract

The use of sustainable materials in geotechnical applications has increased in recent years due to their positive impacts on geo-environmental and future generations. This paper contributes to existing knowledge on geocell reinforcement of soil by proposing a new inexpensive product: cells made from natural materials, Date Palm Leaf fiber coated with Bitumen (DPLB), to improve its durability, as an alternative to commercially available high-density polyethylene (HDPE) geocells. A physical laboratory model was designed to examine the performance of the DPLB cell and HDPE cell reinforced base layer under repeated loading. The study tested different infill materials gravel, sand, and recycled asphalt pavement (RAP) in DPLB cells and HDPLE geocell-reinforced granular layers and compared them to unreinforced layers. The reinforcement's performance was assessed using elastic deformation, permanent deformation, traffic benefit ratio, and rut depth reduction. Results showed that both DPLB cell and geocell reinforced sand decreased the cumulative permanent deformations compared to the unreinforced layer. DPLB reinforcement cells improved the permanent deformation behavior by 30% due to the lateral restriction provided by the DPLB pockets on the infill materials, while the geocell improved it by 7%. The traffic benefit ratio (TBR) of geocell-reinforced RAP is 26% greater than that of the DPLB cell-reinforced RAP section, although both geocell and DPLB cell exhibited similar TBR values in the case of gravel infill materials. The experimental results showed that DPLB cells are a cost-effective and environmentally friendly substitute for commercially available HDPE geocells in soil reinforcement applications.

Keywords: Geocell; Date Palm Leaf Fiber; Permanent Deformation; Repeated Load Test; Elastic Deformation; RAP.

1. Introduction

Shallow foundations constructed over weak subgrade soils often exhibit low bearing capacity and significant settlement. To address these problems, several soil reinforcement techniques have been explored, of which geosynthetic reinforcement has emerged as a prominent solution [1-4]. Geosynthetic reinforcement encompasses planar reinforcement and 3-dimensional interconnected honeycomb cells, known as geocells. The use of geocell is a good solution to improve the weak soil's ability to bear load in different applications like foundation, embankment, slope stabilization, and road applications [5-9].

Nowadays the focus towards the use of sustainable materials has become popular in all aspects of life due to its importance for the environment. It is vital to evaluate the use of sustainable materials in geotechnical applications and investigate their impact on improving soil properties when used as substitute materials for geosynthetic materials [10].

* Corresponding author: cemastura@usm.my

http://dx.doi.org/10.28991/CEJ-2024-010-10-018

Geocells gained prominence dating back to the 1970s when the concept of cellular confinement was first developed [11-15]. In addition to the impact of geocell on improving the bearing capacity of the soil layer, it has been found helpful in reducing settlement, and rutting depth, studies have shown that the percentage of elastic deformation increases with an increasing number of repeated load cycles [16]. Tafreshi & Dawson [17] found that the maximum footing settlement caused by repetitive loading is similar for both planar- and 3D-reinforced sand but significantly better than unreinforced sand settlement. However, increasing the density of reinforcement in the sand led to a decrease in the effectiveness of reinforcement in minimizing the maximum settlement of footing. Overall, the findings demonstrated that the 3-dimensional geotextile reinforcement soil performed better than planar reinforcement in mitigating the effects of dynamic loading using the same mass of geotextile material. Thus, less 3D geotextile material is needed to improve footing settling compared to planar geotextile.

The use of geocell confinements to enhance the efficiency of road layers under cyclic loading has been widely explored. For example, Thakur et al. [18] examined the effects of geocell restriction on recycled asphalt pavement (RAP) layers by using a three-dimensional innovative polymeric alloy (NPA) geocell on a weak subgrade with a target CBR of 2%. The results showed that RAP layers reinforced with geocells had significantly fewer permanent deformations than unreinforced RAP layers when subjected to cyclic plate loading. Geocell confinement enhanced the percentage of elastic deformation and reduced vertical stress distribution at the base-subgrade interface. Another study evaluated the performance of strip footings supported on unreinforced and geocell-reinforced sand beds under static and repeated loads. This study found that geocells effectively decreased the magnitude of final settlement and were more efficient in controlling plastic deformation under repeated loading than static loading [19]. Moreover, the study showed that the effectiveness of geocells in reducing permanent deformation increased with higher reinforcement and loading rates, highlighting their role in enhancing the performance of various foundations under different loading conditions. Khan & Puppala [20] found in their pavement section study that the geocell-reinforced layer reduced the permanent deformation by 36% in comparison to the unreinforced section.

Studies have investigated the efficacy of geocell-reinforced soil under cyclic loading. Saride et al. [21], for instance, used large-scale cyclic models to compare unreinforced and geocell-reinforced sand layers by applying a repeated load between 0.7 and 7 kN on a 150 mm diameter steel footing. They assessed how geocell dimensions affected the cyclic behavior of sand subgrades and discovered that optimizing the geocell geometry reduced rut depth by 75% after 100 cycles, suggesting a significant traffic benefit ratio of 23 at a 10% settlement ratio. Similarly, Biabani et al. [22] assessed the impact of geocell reinforcement on sub-ballast under repeated loading with a regular and positive full-sine wave. They found a correlation between increasing geocell stiffness and a reduction in lateral displacement. Notably, geocells with lower stiffness outperformed those with higher stiffness in terms of limiting lateral displacement. These results provide valuable insights into the effectiveness of geocell reinforcement in mitigating deformations and enhancing the functionality of subgrades under repeated loading conditions. Moreover, Suku et al. [23] studied the impact of geocell reinforcement on unpaved roads, noting a decrease in resilient deformation and the required aggregate layer thickness. Their study also revealed a correlation between higher base layer thicknesses and a significant reduction in permanent deformation. The geocell-reinforced layer showed a noticeable reduction in permanent deformation compared to unreinforced sections [24].

Reinforced layers showed a significant decrease in rut depth compared to unreinforced sections. Additionally, Pokharel et al. [13] studied the effects of geocell reinforcement on the percentage of elastic and permanent deformation in granular layers. Their results implied that geocell reinforcement not only enhanced the proportion of elastic deformation in granular layers but also reduced permanent deformation. They also found that multiple geocell-reinforced sections outperformed single geocell-reinforced portions, highlighting the potential of geocell reinforcement to enhance the structural integrity of granular layers. These results provide valuable insights into the multifaceted benefits of geocell reinforcement in optimizing the behavior of road structures subject to varying load conditions. The rut depth was reduced by about 48.27% with the inclusion of geocell in the base layer as reinforcement materials [25].

In a similar vein, George et al. [26] assessed the efficiency of (HDPE) geocell-reinforced recycled asphalt pavement (RAP). They found geocell confinement increased the traffic benefit ratio, indicating that the geocell-reinforcement layer may sustain larger traffic loads without reaching the same level of rutting as the unreinforced layer. This finding aligns with the work of Rayabharapu & Saride [27], who investigated geocells-reinforced dense sand under repeated loads and found that geocell reinforcement positively impacted repeated load response by increasing the traffic benefit ratio, indicating a significant enhancement in structural behavior. Biswas et al. [28] investigated the behavior of bamboo geocells and jute geocells with three different infill materials: sand, crushed aggregate, and recycled asphalt pavement under a repeated wheel load test. They observed that the jute geocell and bamboo geocell reinforced granular layer increased the traffic benefit ratio significantly, especially the bamboo geocell-reinforced RAP and crushed aggregate can be utilized for low-traffic unpaved roadways.

Typically, the marketed geocells are made from polymer materials such as innovative polymeric alloy and high-density polyethylene, which are expensive and non-environmentally friendly. As a result, current research is focused on identifying environmentally sustainable, economical, and readily available alternative confinement materials. Therefore, geocells made from natural fibers present a cost-effective alternative to polymer-based geocells, potentially leading to cost savings in construction projects. Depending on the specific application, polymer-based geosynthetics can be replaced or substituted with environmentally friendly natural materials. Numerous researchers have investigated the use of different geonatural materials, such as areca leaf sheaths, coir cells, bamboo cells, jute, and sisal cells, as alternatives to HDPE geocell under static load [3, 29-33]. However, there is limited research on the use of natural material in reinforced soil affected by repeated loads. Additionally, previous studies have not provided information on the long-term durability and performance of natural materials treated with coatings to extend their life span.

This study focuses on the necessity of identifying environmentally benign, cost-effective, and readily accessible alternative materials for geocells. The suitability of such technology is contingent on the availability of resources in the area. Arab countries like Iraq, Saudi Arabia, Egypt, and Algeria have enormous natural resource reserves, including date palm leaf fiber. This research assesses the long-term behavior of this natural material in soil confinement. The date palm leaf fiber used in this study was shaped into commercially available geocells, which are naturally abundant. The durability of these date palm leaf cells can be enhanced by coating them with bitumen, which prevents water absorption and fungal growth, thereby extending the product's lifespan. The study also compares the results with those of commercially geocell-reinforced soil. The subsequent investigation reports findings from model footing tests performed on i) an unreinforced subgrade layer, ii) a geocell-reinforced subgrade layer, and iii) a date palm leaf-coated bitumen cell-reinforced subgrade layer under repeated loading.

2. Material and Methods

High-density polyethylene geocell (HDPE) was used as soil reinforcement; date palm leaf fiber was used as cellular confinement for soil after being coated with bitumen and then sewn and designed in pockets similar to geocell pockets; clay was used as subgrade soil; and sand, gravel, and recycled asphalt pavement (RAP) were used as base materials for the physical model. Geotextile was used as a separate layer between the subgrade and base layers. The general methodology of the work is shown in the flowchart in Figure 1.

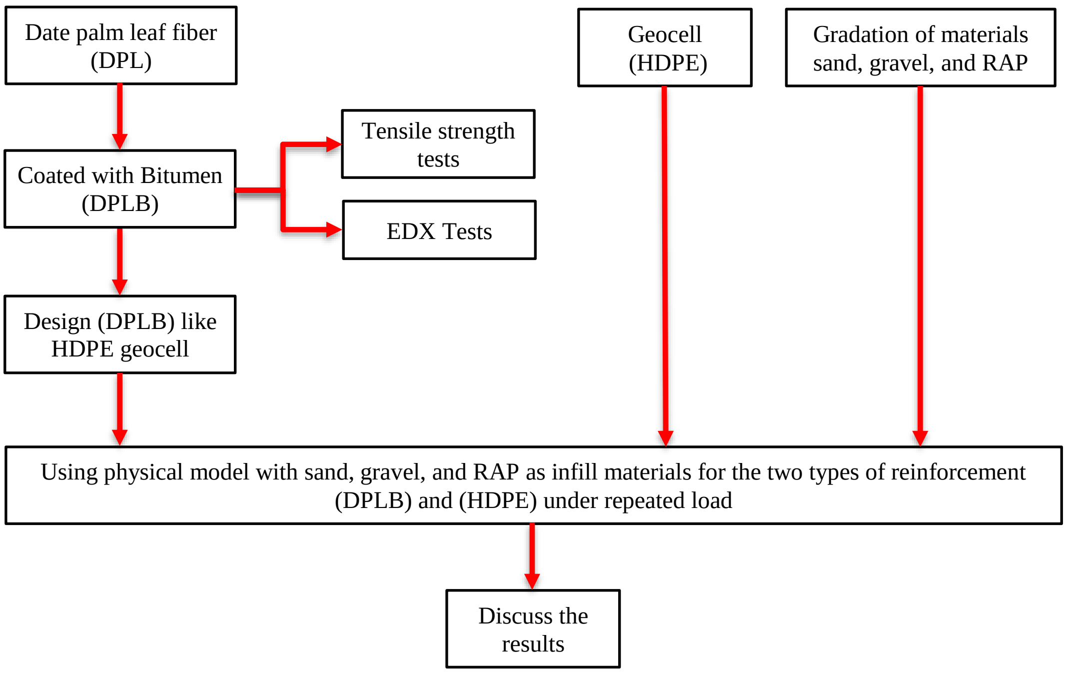

Figure 1. Flowchart of the experimental methodology

2.1. Date Palm Leaf Fiber Cells and Coating Materials

Date palm leaf, used as a substitute for HDPE geocell, might be produced by keeping a similar HDPE geocell pocket size. The PDL fiber was immersed in water for 10 minutes, sliced into 10 mm strips, which were handmade and woven into mats. To protect against environmental damage when used as cellular confinement in the soil and enhance tensile strength, the DPL was coated with bitumen, a thick, sticky liquid substance derived from an oil reservoir. Bitumen, a low-grade crude oil with a complex, heavy hydrocarbon composition, is the primary fossil fuel component of oil sands [34]. The bitumen utilized in this study, known as bituproof, has a viscosity of 40 g/ltr and is identified as Bitumen Type 40S Bitumen, a cold emulsified black/brown liquid. This bitumen serves as a moisture- and vapor-resistant barrier for concrete and masonry and acts as a general-purpose primer for bituminous membranes. Figure 2 shows the coated DPL cells used in this study. Generally, bitumen is a plentiful and inexpensive substance with a substantial, proven global reserve of over three metric tons. Bitumen coatings are viscous substances that demonstrate exceptional durability against industrial pollutants. Also, bitumen with well-defined characteristics and capabilities is currently utilized in various coating forms, including enamels, bituminous wrappings, bituminous tapes, and bituminous paints. These coatings are employed to protect steel and other structural materials in industries that are subject to corrosion, such as petroleum, chemical, and water industries.

Figure 2. The DPL cells used in this research

The tensile strength of the HDPE geocell material, untreated and treated date palm leaf fiber, was tested according to the ASTM D6637-01 standard using the multi-rib tensile method for geogrids. A 400 mm long, 50 mm wide, and 2 mm thick sample of woven treated and untreated DPLB fiber was tested at a rate of 5 mm per minute, consistent with ASTM D6637 specifications. The speed of the tensile test machine will be 5 mm/min. Results showed the maximum tensile strength of the bitumen coating DPL fiber is two times greater as compared with the polyurethane coating DPL fiber and untreated DPL fiber. As well as the treated date palm leaf fiber, the maximum tensile strength was 1.5 times higher than that of the HDPE geocell. Additionally, Figure 3 illustrates that the strain percentage was also higher in the date palm leaf fiber mat than in the HDPE geocell.

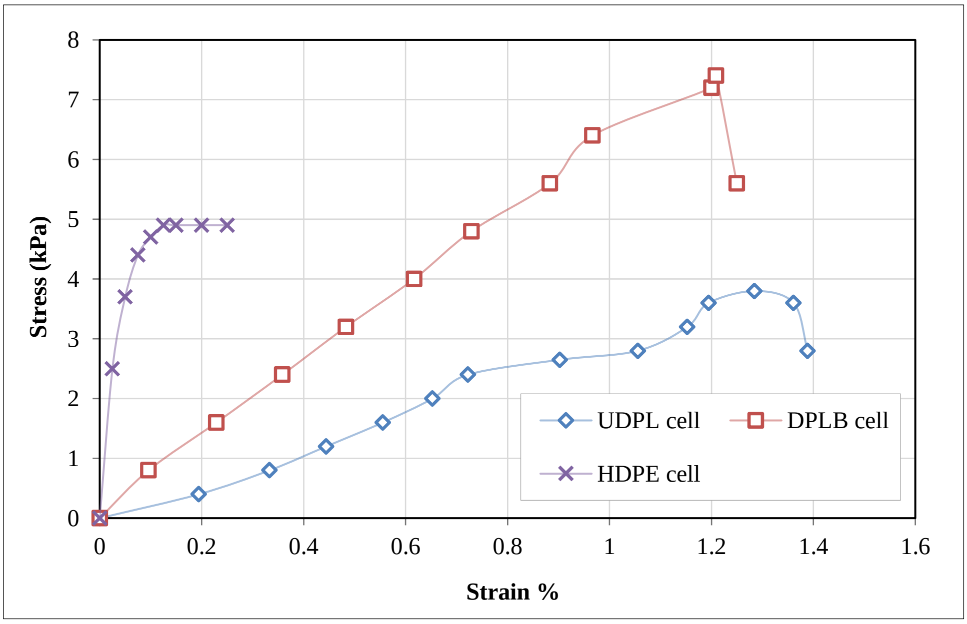

Figure 3. Tensile stress-strain behavior of materials

Table 1 summarizes the results of the EDX test. The results reveal that the durability treatment procedure used is very effective for this type of material, where the percent of oxygen to carbon (O/C) increased from 0.215 for the untreated DPL fiber to 0.802 for the treated DPL fiber with bitumen, indicating that the treatment helped in removing impurities and consequently improving the durability of the DPL fiber.

Table 1. Chemical composition of treated and untreated DPL fiber

Element	Atom. C (wt.%)	
	Untreated DPL fiber	DPL fiber treated with bitumen
Oxygen	16.73	8.88
Carbon	77.77	11.07
Silica	3.04	0.73
Iron	1.02	0.44
Aluminium	0.80	0.24
Magnesium	0.64	0.14
Hydrogen	-	77.46
Sodium	-	0.45
Nitrogen	-	0.50
Sulphur	-	0.09

2.2. Geocell and Geotextile

This research used a geocell fabricated of high-density polyethylene (HDPE) (MTS FIBROMAT, Malaysia). HDPE has a density of 0.94 g/cm^3 and can resist environmental stress cracking for up to 1500 hours. The geocell dimensions were 100 mm in height, 1.2 mm in sheet thickness, and an internal dimension of 203 mm x 244 mm when expanded as shown in Figure 4. For both reinforced and unreinforced parts, geotextile was used beneath the geocell, although its effect was not analyzed in this research, which focuses on comparing DPLB cell reinforcement and geocell reinforcement with the unreinforced sections. However, geotextile serves as a separation of overall test sections. The geotextile material's features are summarized in Table 2.

Figure 4. The HDPE utilized in this study

Table 2. Characteristics of geotextile material

Materials characteristics		Standard	Value
Mass /units area (gms/m^3)		ASTM D5261 [35]	200
Thickness (2Kn/m^2)		ASTM D5199 [36]	1.5
Grab tensile strength (N)	MD	ASTM D4632 [37]	750
	CD		700
Grab tensile Elongation (%)	MD	ASTM D4632 [38]	>50
	CD		>50
Trapezoidal Tear strength (N)	MD	ASTM D4632 [38]	280
	CD		250
CBR puncture strength (N)		ASTM D6241 [39]	2200
Apparent Opening Size(O_{90}) (microns)		ASTM D4751 [40]	80
Permittivity (s^{-1})		ASTM D4491 [41]	1.6
UV resistance (at 150 hrs.)		ASTM D4355 [38]	>85
Flow rate- 5 cm head		ASTM D4491 [42]	l/m^2/s

2.3. Subgrade Material and Base Materials

The clayey soil, used as the subgrade, was collected from a site in the Dagharah region of Alqadissyah, southern Iraq, at a depth of about 1 meter. Soil compaction was done according to standard test methods (ASTM D 698) [42] to determine the optimum moisture content and maximum dry density, which were 23.9% and 16.8 kN/m², respectively. Sand, gravel, and recycled asphalt pavement (RAP) were used as infill materials for the base layer. The sand, sourced locally, was a cheaper material classified as SW in the Unified Soil Classification System (USCS). The models tested using the constant height of fall method maintained a relative density of 70% throughout the test. Aggregated and RAP were the second and third infill materials, respectively, used. The grain size distribution was in accordance with the state corporation for roads and bridges in Iraq [43], which produced base course standard requirements. Table 3 presents the gradation materials, while Figure 5 shows the grain size distribution curves of base materials.

Table 3. Gradation of materials

Sieve size	Sieve opening (mm)	Percentage passing by weight of total aggregate		
		Base course		
		Specification limit (S.C.R.B)	Selected gradation of aggregate	Selected gradation of RAP
1 ½”	37.5	100	100	100
1"	25.0	80-100	95	100
½"	12.5	50-80	70	80
No. 4	4.75	30-60	47	30
No. 40	0.425	10-30	22	10
No. 200	0.075	5-15	10	5

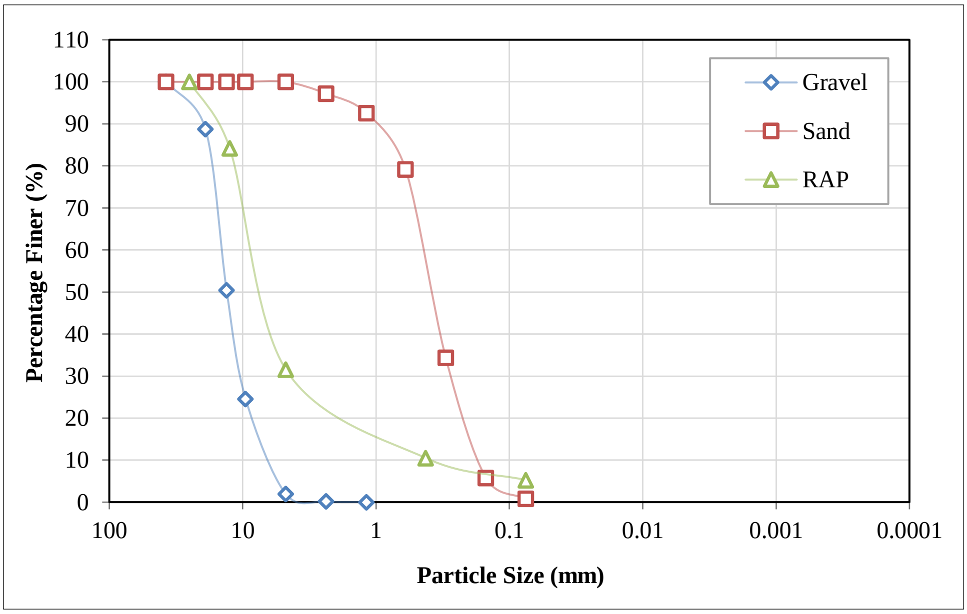

Figure 5. Grain size distribution curves of sand, gravel, and RAP material

2.4. Test Equipment and Setup

A specially designed, medium-sized loading apparatus was used to conduct repeated load tests and assess the HDPE performance and DPL reinforcement. The loading plate had a diameter of 150 mm, and the square test box measured 800 x 800 x 600 mm with two absorbing layers: a rubber layer and a polystyrene layer. The setup also comprised linear variable displacement transducers (LVDTs), a data acquisition system, an accumulator, a hydraulic pump, and a cyclic load regulator. A laboratory testing setup and schematic layout are shown in Figure 6. This study used a hydraulic fluid pumped into a vertical actuator via a servo control unit to apply repeated load cycles on the loading plate. The hydraulic fluid was cycled by a flow control system, comprising an accumulator and hydraulic pump that were coupled to the servo control unit. The accumulator was subjected to a constant high pressure of 18 MPa throughout the repeated load tests. Two LVDTs measured displacement at the loading plate's surface, and a load cell on the loading shaft measured the axial load. The data from the load cell and LVDTs were transferred to the data acquisition system.

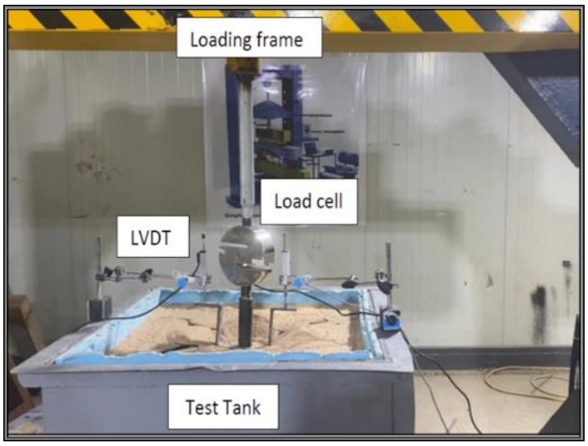

(a)

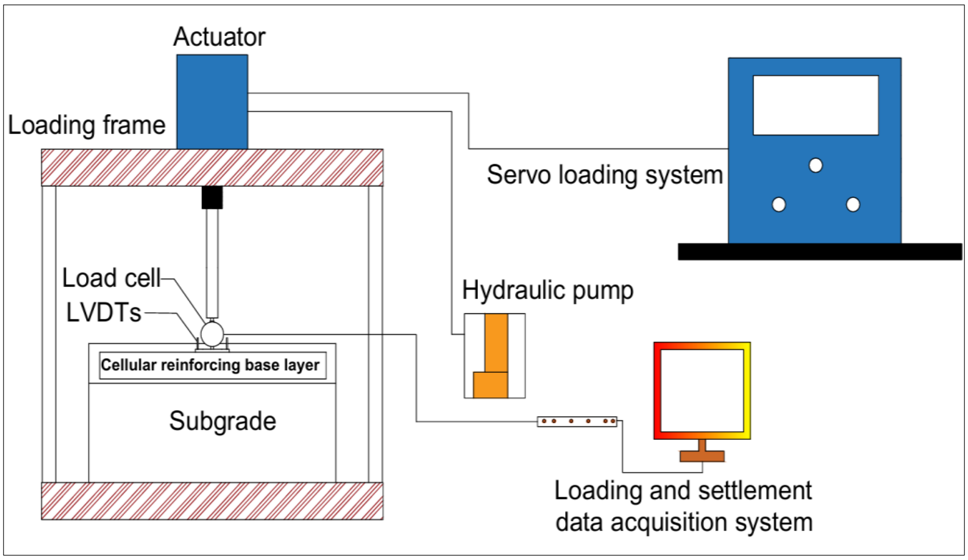

(b)

Figure 6. Laboratory testing setup. b. Schematic layout of the laboratory setup

Each test section had a 450 mm clay subgrade compacted to 95% of the maximum dry density (MDD) with moisture content at the optimum water content (OMC). The subgrade was set in six 75 mm lifts, each of which was compacted with a hand-compacted hammer to achieve the required dry density. A non-woven geotextile was placed as a barrier between the base layer and subgrade to prevent material penetration during loading. The cellular reinforcement system was 100 mm high with a 20 mm thick fill cover made of the same material as the infill material. This ensured equal or uniform compaction of the infill material in the cells' pockets and ensured uniform distribution of the load on the top layer of the cellular reinforcement. In all tests, the reinforcement cells were filled with the infill material, and the sand was compacted to 70% relative density inside and outside the cell in three layers: two 50 mm thick layers and one 20 mm cover layer. As mentioned in section 2.3, the gravel and RAP gradation matched the standards of the state corporation for roads and bridges in Iraq. The load was used at an average frequency of 0.05 Hz with a minimum load of 0 kN and a maximum load of 9.5 kN to simulate the traffic loading pattern.

2.5. Experimental Program

Nine laboratory tests were carried out in three groups based on the type of infill material (sand, gravel, and RAP). Each test group had three sections: unreinforced, reinforced with HDPE geocell, and reinforced with DPLB cell. The test involved applying the repeated load at a frequency range of 0.05 Hz, with the loading plate positioned at the center of the box for the unreinforced case or the middle of the cell for the reinforced case. The load gradually increased from 0 kN to a maximum of 9.5 kN over 4 seconds, maintained at the maximum for 1.5 seconds, and then slowly decreased back to the minimum load over 3.5 seconds. This minimum load was maintained for 11 seconds before the next cycle again. Testing continued until the elastic deformation percentage stabilized after many loading cycles. The performance of the reinforcement on the base layer was evaluated by measuring the permanent deformations and the test bed's resilient modulus. The applied axial load and total surface deformation were measured using a load cell and two LVDTs at 0.1-second intervals. The overall surface deformation at the loading plate’s center was calculated by averaging the deformation data from the two LVDTs positioned on the loading plate's surface.

3. Results and Discussion

Before the repeated loading tests, the potential impact of the test box boundaries and the test results were evaluated. Previous research indicated that an 800 mm × 800 mm box was sufficient to eliminate boundary effects [13]. Two layers of absorbing materials, including rubber and polystyrene, were placed on one side of the box to minimize wave absorption. Subsequent tests assessed the performance of unreinforced, geocell-reinforced, and DPLB-reinforced layers using sand, gravel, and RAP infill materials under repeated loading conditions. The test results are discussed in the subsequent sections.

3.1. Elastic Deformation (Resilient Deformation) (ED)

The elastic deformation of the test bed surface under repeated loading was determined using the rebound curve during the unloading of each load cycle [18, 26]. Figure 7 illustrates the relationship between resilient deformation and the number of cycles for unreinforced sand, geocell-reinforced sand, and DPLB-reinforced sand. The findings indicate that DPLB-reinforced sand exhibits 1.5 times less resilient deformation than the unreinforced sand, while the geocell-reinforced sand exhibits 1.2 times less resilient deformation than the unreinforced sand. This suggests that the cellular reinforced layers have more elastic responses than the unreinforced layers due to the inclusion of cellular confinement, aligning with previous results [13].

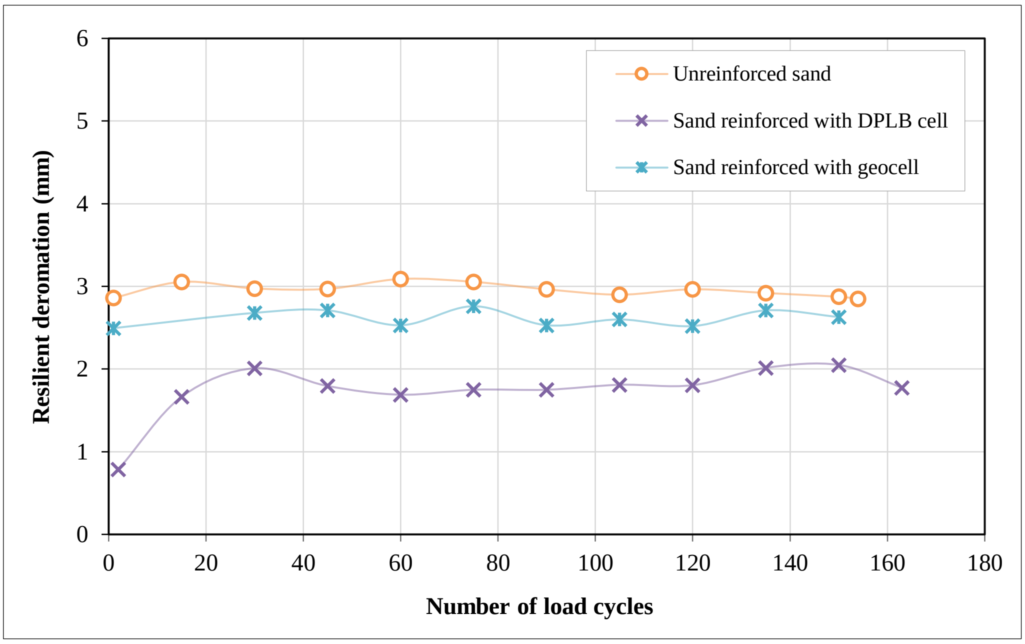

Figure 7. Resilient deformation versus number of load cycles for sand layers

Figure 8 depicts resilient deformation at the center of the loading plate versus the number of cycles for unreinforced RAP, geocell-reinforced RAP, and DPLB-reinforced RAP. Resilient deformation increased rapidly during the initial loading cycles but quickly reached a steady state for layers reinforced with DPLB cells. The elastic deformations for geocell-reinforced layers stabilized after 60 cycles, showing largely resilient responses. Results indicate that the DPLB-reinforced RAP exhibited 1.2 times less resilient deformation than the unreinforced RAP, while the geocell-reinforced RAP exhibited 1.8 times less resilient deformation than the unreinforced RAP. This suggests that the lateral confinement provided by the DPLB cell reinforcement significantly enhanced the resilient behavior of the RAP base, consistent with previous findings by George et al. [26], which have concluded that the elastic deformation for 10 cm geocell-reinforced RAP evidence 2.2 times less compared to the unreinforced layer after 500 cycles.

Figure 9 shows that both geocell-reinforced gravel and DPLB-reinforced gravel have lower resilient deformations than the unreinforced section. The reinforced sections show 1.4 times less resilient deformation than the unreinforced gravel base, indicating similar lateral confinement provided by both DPLB cell-reinforced and geocell-reinforced gravel bases. This confinement significantly improves the resilient behavior of the gravel base section, an observation consistent with results of previous research [23], which have concluded that the resilient deformation for the layer of 300 mm thickness reinforced with geocell exhibits 1.6 times less in comparison to the unreinforced layer.

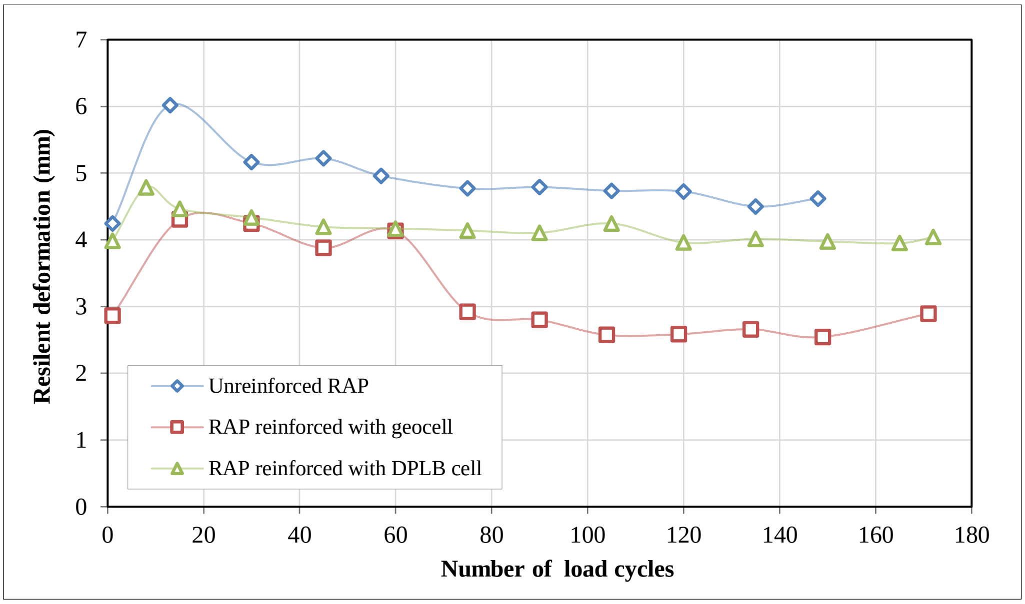

Figure 8. Resilient deformation versus number of load cycles for RAP layers

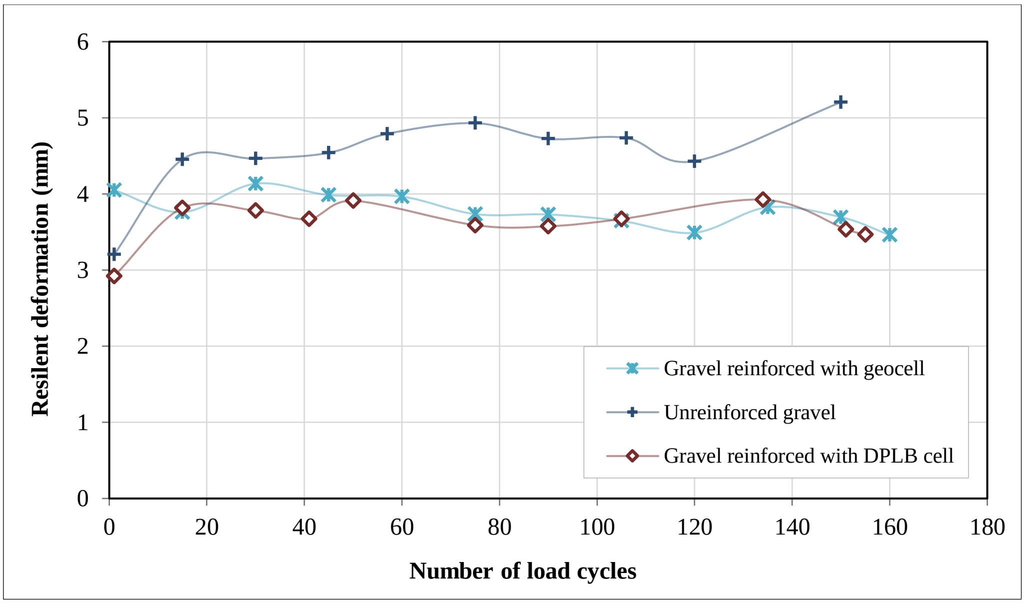

Figure 9. Resilient deformation versus number of load cycles for gravel layers

The results from this study demonstrate that the DPLB cell reinforcement improved the resilient behavior in comparison with the HDPE geocell. It can be deduced that the DPLB cell-reinforced sand can perform much better than the unreinforced base under repeated loading, which could be attributed to the confining by the cellular framework.

3.2. Cumulative Permanent Deformation (PD)

Cumulative permanent deformation, also known as plastic deformation, is the accumulation of irreversible deformation in a material under loading over time, which can result in permanent damage [21]. Figure 10 depicts the relationship between cumulative permanent deformation and the number of load cycles of unreinforced, geocell-reinforced, and DPLB-reinforced sand layers. It shows that as the number of load cycles increases, the permanent deformation in both reinforced and unreinforced sand sections increases. A significant increase in permanent deformations occurs up to 120 load cycles, after which it stabilizes. However, both geocell and DPLB cell-reinforced sand reduce the cumulative permanent deformations compared to the unreinforced sand section, consistent with earlier research findings [21]. Specifically, DPLB reinforcement cells improve permanent deformation behavior by 30% due to lateral confinement provided by DPLB pockets, while geocell reinforcement shows a 7% improvement due to less lateral confinement, which allows sand to escape through openings in the geocell walls. Cellular reinforcement mechanism in two ways: the reinforcement and the separation, which are the techniques of enhancing weak soil by the inclusion of geocell to increase the stiffness and the soil's ability to bear load by frictional interaction between the cellular reinforcement materials and soil. Undoubtedly, the reason for this behavior is attributed to the stronger and stiffer of these reinforcing materials, which give more strength than the equivalent soil without reinforcement. Therefore, cellular reinforcement enhanced the interlocking of aggregate in sustaining road systems throughout subbase restraint reinforcement. Furthermore, cellular reinforcement between the base course and subgrade soil supports the shear stress that vehicular loads induce. In general, cellular confinement reinforces the subbase or subgrade materials by providing lateral confinement (reducing spread), tensile membrane support, and an improvement in load-bearing ability.

Figure 11 presents the cumulative permanent deformation versus load cycles of unreinforced, geocell-reinforced, and DPLB cell-reinforced RAP layers. Increased permanent deformation is observed in both reinforced and unreinforced RAP layers with more load cycles. However, reinforced sections show significant deformation only up to 100 cycles, after which it stabilizes, while unreinforced sections continue to deform with increasing load cycles. This indicates that geocell and DPLB cell reinforcements reduce cumulative permanent deformation by 10% compared to unreinforced RAP base due to the lateral confinement provided by the cellular pockets on the infill RAP materials. The enhanced effectiveness may be attributed to the tension beam (membrane) effect Thakur et al. [18] wherein the cellular reinforcement faced tensile force when subject to repeated load. As a result, an area of tension is at the bottom part of the cellular reinforcement system, and then this enhances the structural support, leading to a decrease in the vertical deformation of the subgrade. This signifies the importance of cellular confinement in enhancing RAP base performance over the unreinforced section. As noted in similar studies [26], they found that the application of 10-cm and 15-cm geocell reinforcement enhanced the permanent deformation of RAP base by 70-80% after 500 cycles.

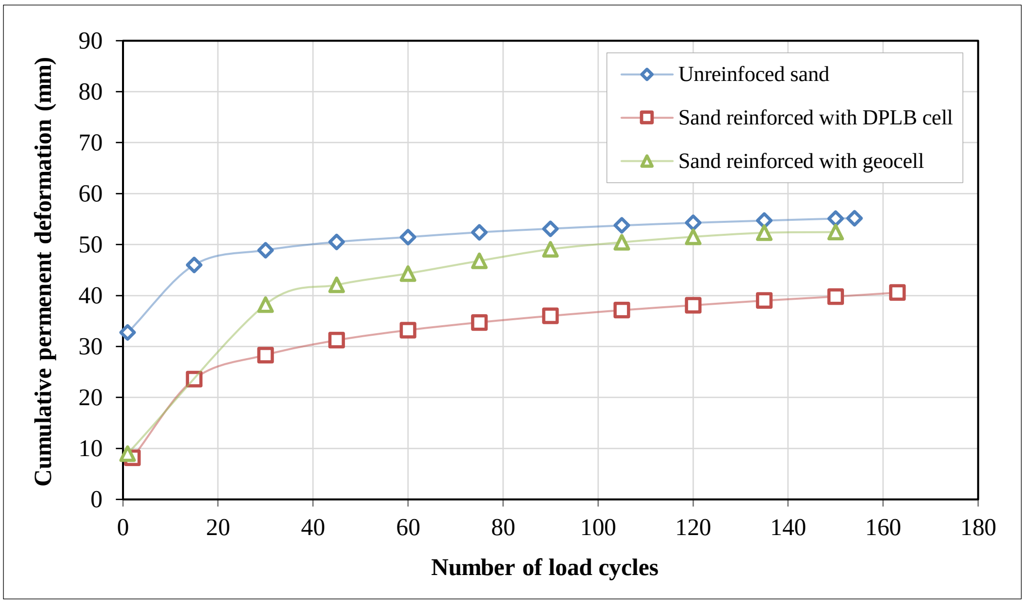

Figure 10. Cumulative permanent deformation versus the number of load cycles for sand layers

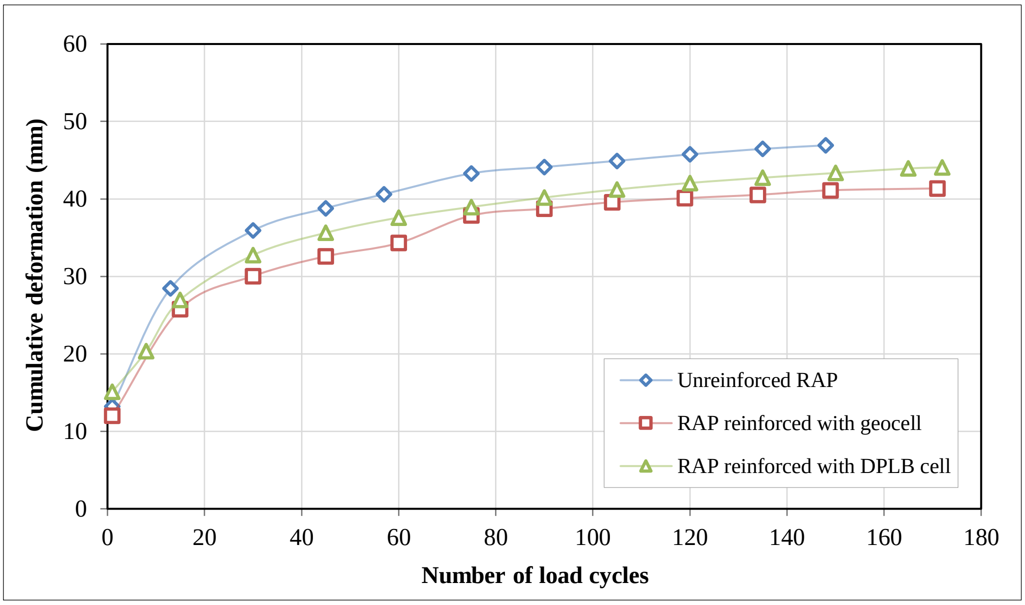

Figure 11. Cumulative permanent deformation versus the number of load cycles for RAP layers

Figure 12 illustrates the permanent deformations and number of cycles of the unreinforced, geocell-reinforced, and DPLB cell-reinforced gravel layers. Initially, the permanent deformation for the reinforced section is slightly higher until 40 load cycles, after which it stabilizes to a lower value as evidenced by the compression between the reinforced and unreinforced. DPLB cell reinforcement enhances permanent deformation behavior by 30%, whereas the geocell reinforcement improved it by 40%. Studies have shown a notable increase in total deformation with an increasing number of cycles for both reinforced and unreinforced sections, with less deformation observed in the reinforced section than in the unreinforced section [23], where the permanent deformation of the latter reached 63 mm.

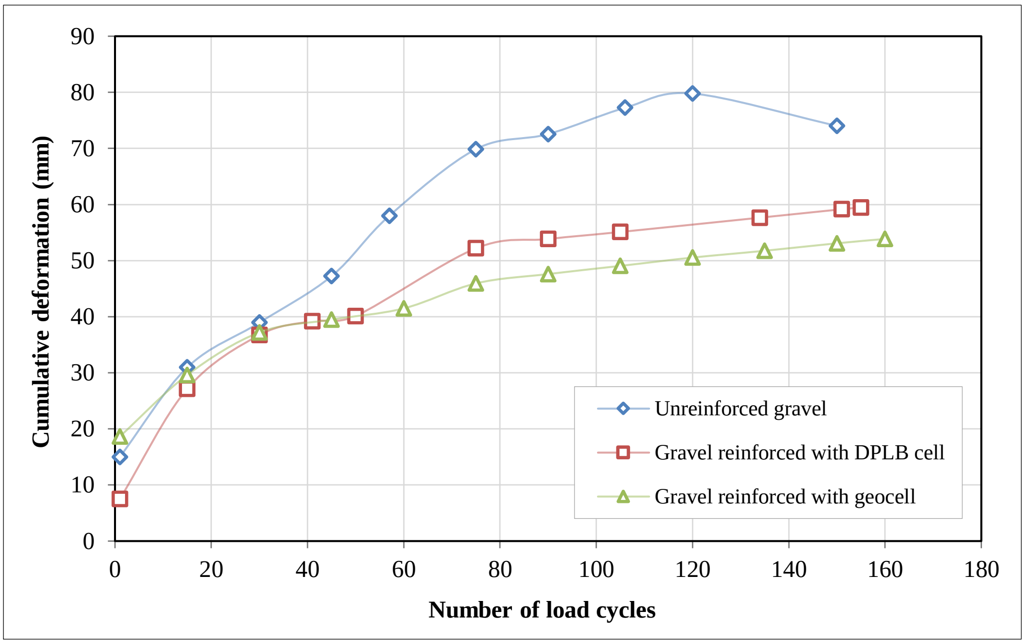

Figure 12. Cumulative permanent deformation versus the number of load cycles for gravel layers

Overall, the findings on permanent deformation have shown that under repeated loading of the same magnitude, reinforced layers exhibit significantly reduced permanent deformation across all infill materials compared to unreinforced layers, an observation that aligns with earlier research results [13].

3.3. Traffic Benefit Ratio (TBR)

The benefit of confinement reinforcement for increasing pavement life can be quantified using the traffic benefit ratio, a dimensionless index. TBR is characterized by comparing the difference between the frequency of load cycles needed for the reinforced test section to reach the same level of rutting depth (i.e., permanent deformation) and the unreinforced test section. The ratio, also known as the traffic improvement factor, is calculated as follows:

$$TBR = \frac{Nr}{Nu} \tag{1}$$

where Nu is the number of load cycles for the unreinforced section, and Nr is the number of load cycles on the reinforced section. The benefit of confinement reinforcement in the sand was significantly higher than those of the stronger materials such as gravel and RAP; hence, the TBR values for the sand section were not computed. Figure 13 illustrates the variation in TBR with the number of load cycles for RAP and gravel. The TBR increases with cumulative permanent deformations in all cellular reinforcement. The general trend shows an increase in TBR up to 35 mm cumulative permanent deformations for all cellular confinement-reinforcement models. This is likely due to the increase in rut depth in the weak subgrade of the unreinforced models [44]. The TBR value of geocell-reinforced RAP is 30% greater than that of the DPLB cell-reinforced RAP section, while both geocell and DPLB cell exhibit similar TBR values with gravel infill materials. The shear stress generated between the soil particles and the cellular confinement materials enhances the lateral confinement stress within the base layer. In contrast, granular materials generally show an increase in elastic modulus with increased confining stress. Furthermore, the second reinforcement component results from an increase in stiffness of the base (or subbase) coarse aggregate when sufficient interaction develops between the soil and the cellular confinement materials. As a result, the increased stiffness of this layer results in lower vertical strains in the soil. A similar trend was also observed by Biswas et al. [28], in which the TBR of the jute geocell and bamboo geocell-reinforced granular layer increased (1-2) and (3-5) times at a rut depth equal to 50 mm, respectively.

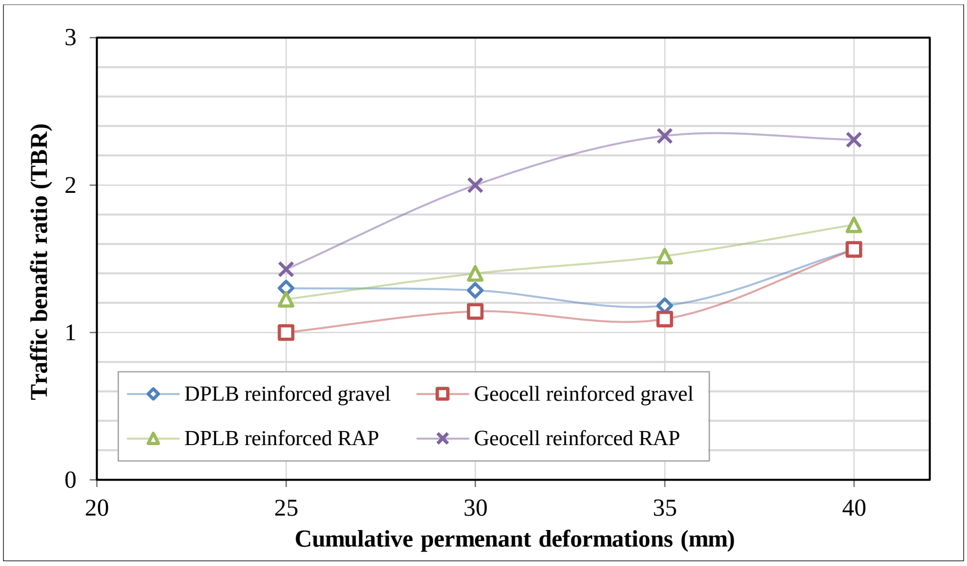

Figure 13. Traffic benefit ratio varies the number of load cycles for RAP and gravel layers

3.4. Rut Depth Reduction (RDR)

Rut depth reduction measures the performance enhancement of reinforcement compared to unreinforced sections under repeated loading. RDR is calculated by the ratio of the difference in cumulative permanent deformation between reinforced and unreinforced sections for a specific number of load cycles [21] as shown in Equation 2:

$$(RDR)_{N=n} = \left(1 - \frac{Dr}{\mathrm{Du}}\right)_{N=n} \times 100 \tag{2}$$

The rut depth reduction for different cellular reinforcements and infill materials was measured at many load cycles, with results displayed in Figure 14. The RDR is calculated every 15 cycles, starting from 75 cycles. The results show that RDR values are approximately constant values of 27.7% and 4.8% for DPLB cell and geocell-reinforced sand base, respectively. The RDR values are approximately 8% and 11.8% constant for the DPLB cell and geocell-reinforced RAP base, respectively. In the case of gravel base, RDR initially increases to 37% and 30% for geocell and DPLB cell reinforcement, respectively, then decreases to 28% and 20% at the end of load cycles. In all scenarios, the RDR rate declines as the number of cycles increases, due to the reduced permanent deformation rate from the densification of the reinforced layer. Studies have reported that geocell-reinforced gravel and RAP base sections perform significantly better in rut depth reduction compared to their unreinforced counterparts [23, 26].

Figure 14 shows that at the end of cycles, geocell-reinforced gravel and DPLB cell-reinforced sand have the highest RDR of approximately 28%. This observation aligns with field experimental results from Tabatabaei et al., where the geocell reinforcement reduced the rutting depth by 20% after 40 passes [45]. Önal et al. found that geocell reinforcement in a sand base layer provided an RDR of 48.27% after 2000 load cycles [25].

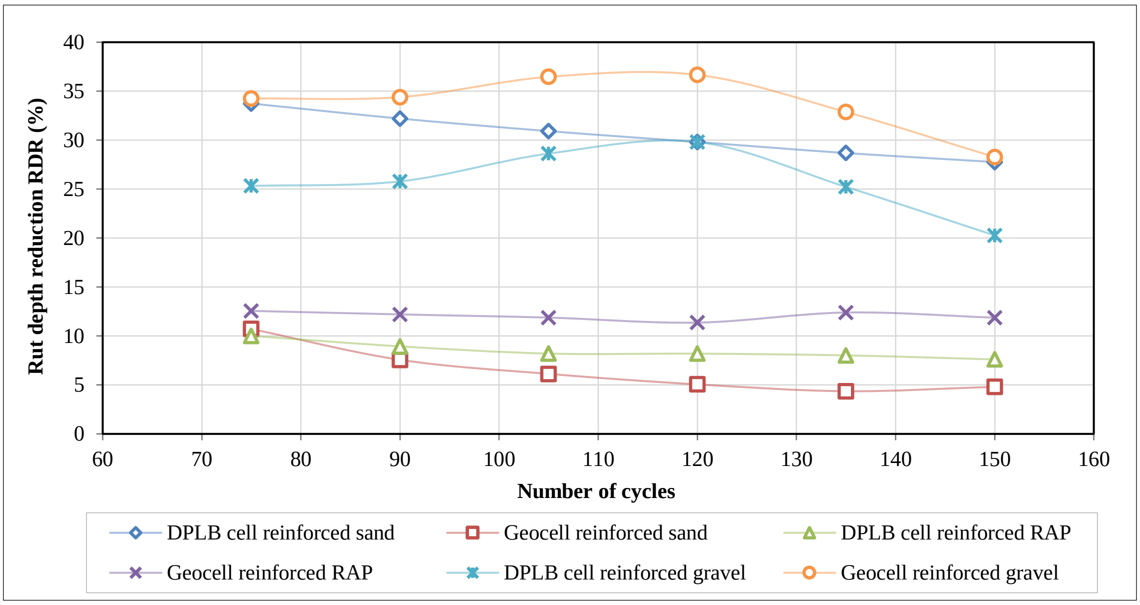

Figure 14. Rut depth reduction varies with the number of load cycles for the sand, RAP, and gravel base sections

4. Conclusions

This research investigated the behavior of a new type of cellar reinforcement (DPLB cells) in reinforced soil layers under repeated loading, comparing them with commercially available HDPE geocells Three types of granular materials (sand, gravel, and RAP) were used as infill for both reinforced and unreinforced sections as reference points. All cases were subjected to repeated loading to assess the benefits of reinforcement in terms of resilient deformation, cumulative permanent deformation, traffic benefit ratio (TBR), and rut depth reduction (RDR). The following conclusions were obtained:

- The tensile strength of the date palm leaf fiber mat coated with bitumen was found to be 1.5 times greater than that of HDPLE geocell material. Given that the strain percentage is greater in the DPLB fiber mat; it is recommended for use in high-strain geotechnical applications. The reinforcement significantly reduced the permanent deformation under repeated loading in contrast to the unreinforced layers for all three infill materials. DPLB cells-reinforced sand also showed a significant reduction in permanent deformation, unlike the HDPE geocells.
- Moreover, both geocell and geo-natural cell reinforced sand layers reduced the cumulative permanent deformations compared to the unreinforced sand layer. DPLB reinforcement cells improved the permanent deformation behavior by 30% due to the lateral confinement provided by geo-natural cells on the filling materials, while the geocell enhanced this behavior by 7%.
- The traffic benefit ratio of geocell reinforced RAP was 36% greater than DPLB cell reinforced RAP section, while both geocell and DPLB cell exhibited similar behaviour in terms of TBR value for gravel infill materials. DPLB cells emerged as a highly economical and environmentally friendly alternative to commercially available HDPE geocells for soil reinforcement and cellular confinement. This research utilized man-made DPLB cells, designing machinery to produce these DPLB cells from palm leaf can help ensure the uniformity and quality of these products in practical applications.

However, the manufacture and scaling of DPLB cells for commercial purposes are faced with numerous obstacles. These issues are linked to the need to develop efficient manufacturing procedures or processes to ensure the constant quality and performance of DPLB cells. Hence, to expand the production of DPLB cells, it is important to address these problems by implementing innovative, cost-effective processing methods and ensuring both environmental and economic sustainability.

5. Declarations

5.1. Author Contributions

Conceptualization, N.S.A. and M.A.; methodology, N.S.A. and M.Y.F.; investigation, N.S.A. and M.A.; data curation, N.S.A.; writing—original draft preparation, N.S.A.; writing—review and editing, M.A. and M.Y.F.; visualization, N.S.A.; supervision, M.A., F.A., and M.Y.F.; funding acquisition, N.S.A. All authors have read and agreed to the published version of the manuscript.

5.2. Data Availability Statement

The data presented in this study are available in the article.

5.3. Funding

The authors received no financial support for the research, authorship, and/or publication of this article.

5.4. Conflicts of Interest

The authors declare no conflict of interest.

6. References

[1] Michalowski, R. L. (2004). Limit Loads on Reinforced Foundation Soils. Journal of Geotechnical and Geoenvironmental Engineering, 130(4), 381–390. doi:10.1061/(asce)1090-0241(2004)130:4(381).

[2] Chao, S.-J. (2008). Performance study on geosynthetic reinforced shallow foundations. International Conference on Case Histories in Geotechnical Engineering, 11-16 August, 2008, Arlington, United States.

[3] Lal, D., Sankar, N., & Chandrakaran, S. (2017). Behaviour of square footing on sand reinforced with coir geocell. Arabian Journal of Geosciences, 10(15). doi:10.1007/s12517-017-3131-9.

[4] Jaiswal, S., Srivastava, A., & Bhushan Chauhan, V. (2021). Improvement of Bearing Capacity of Shallow Foundation Resting on Wraparound Geotextile Reinforced Soil. IFCEE 2021, 65–74. doi:10.1061/9780784483411.007.

[5] Mishra, B. (2016). A Study on Ground Improvement Technique and it's an application. International Journal of Innovative Research in Science, 5(1), 72–86. doi:10.15680/IJIRSET.2015.0501010.

[6] Hegde, A. (2017). Geocell reinforced foundation beds-past findings, present trends and future prospects: A state-of-the-art review. Construction and Building Materials, 154, 658–674. doi:10.1016/j.conbuildmat.2017.07.230.

[7] Ghani, S., Kumari, S., & Choudhary, A. K. (2024). Geocell Mattress Reinforcement for Bottom Ash: A Comprehensive Study of Load-Settlement Characteristics. Iranian Journal of Science and Technology - Transactions of Civil Engineering, 48(2), 727–743. doi:10.1007/s40996-023-01205-8.

[8] Luo, X., Lu, Z., Yao, H., Zhang, J., & Song, W. (2022). Experimental study on soft rock subgrade reinforced with geocell. Road Materials and Pavement Design, 23(9), 2190–2204. doi:10.1080/14680629.2021.1948907.

[9] Banerjee, S., Manna, B., & Shahu, J. T. (2024). Geocell as a Promising Reinforcement Technique for Road Pavement: A State of the Art. Indian Geotechnical Journal, 54(4), 1644–1665. doi:10.1007/s40098-023-00818-0.

[10] Al-Hassnawi, N. S., Ahmad, F., Fattah, M. Y., & Azmi, M. (2024). Review of Natural Fiber Application for Sustainable Ground Improvement. Proceedings of AWAM International Conference on Civil Engineering 2022 - Volume 3, AICCE 2022, Lecture Notes in Civil Engineering, 386. Springer, Singapore. doi:10.1007/978-981-99-6026-2_10.

[11] Rajagopal, K., Krishnaswamy, N. R., & Latha, G. M. (1999). Behaviour of sand confined with single and multiple geocells. Geotextiles and Geomembranes, 17(3), 171–184. doi:10.1016/S0266-1144(98)00034-X.

[12] Yang, X. (2010). Numerical Analyses of Geocell- Reinforced Granular Soils under Static and Repeated Loads. PhD Thesis, University of Kansas, Lawrence, United States.

[13] Pokharel, S. K., Han, J., Leshchinsky, D., & Parsons, R. L. (2018). Experimental evaluation of geocell-reinforced bases under repeated loading. International Journal of Pavement Research and Technology, 11(2), 114–127. doi:10.1016/j.ijprt.2017.03.007.

[14] Sheikh, I. R., & Shah, M. Y. (2020). Experimental study on geocell reinforced base over dredged soil using static plate load test. International Journal of Pavement Research and Technology, 13(3), 286–295. doi:10.1007/s42947-020-0238-2.

[15] Fattah, M. Y., Zbar, B. S., & Al-Kalali, H. H. M. (2023). Experimental Investigation of the Performance of Buried Flexible Pipe in Reinforced Sand. Slovak Journal of Civil Engineering, 31(2), 48–60. doi:10.2478/sjce-2023-0012.

[16] Pokharel, S. K., Han, J., Leshchinsky, D., Parsons, R. L., & Halahmi, I. (2009). Behavior of Geocell-Reinforced Granular Bases under Static and Repeated Loads (pp. 409–416). doi:10.1061/41023(337)52.

[17] Tafreshi, S. N. M., & Dawson, A. R. (2010). Behaviour of footings on reinforced sand subjected to repeated loading - Comparing use of 3D and planar geotextile. Geotextiles and Geomembranes, 28(5), 434–447. doi:10.1016/j.geotexmem.2009.12.007.

[18] Thakur, J. K., Han, J., Pokharel, S. K., & Parsons, R. L. (2012). Performance of geocell-reinforced recycled asphalt pavement (RAP) bases over weak subgrade under cyclic plate loading. Geotextiles and Geomembranes, 35, 14–24. doi:10.1016/j.geotexmem.2012.06.004.

[19] Moghaddas Tafreshi, S. N., & Dawson, A. R. (2012). A comparison of static and cyclic loading responses of foundations on geocell-reinforced sand. Geotextiles and Geomembranes, 32, 55–68. doi:10.1016/j.geotexmem.2011.12.003.

[20] Khan, M. A., & Puppala, A. J. (2023). Sustainable pavement with geocell reinforced reclaimed-asphalt-pavement (RAP) base layer. Journal of Cleaner Production, 387, 135802. doi:10.1016/j.jclepro.2022.135802.

[21] Saride, S., Rayabharapu, V. K., & Vedpathak, S. (2015). Evaluation of Rutting Behaviour of Geocell Reinforced Sand Subgrades Under Repeated Loading. Indian Geotechnical Journal, 45(4), 378–388. doi:10.1007/s40098-014-0120-8.

[22] Biabani, M. M., Indraratna, B., & Ngo, N. T. (2016). Modelling of geocell-reinforced subballast subjected to cyclic loading. Geotextiles and Geomembranes, 44(4), 489–503. doi:10.1016/j.geotexmem.2016.02.001.

[23] Suku, L., Prabhu, S. S., Ramesh, P., & Babu, G. L. S. (2016). Behavior of geocell-reinforced granular base under repeated loading. Transportation Geotechnics, 9, 17–30. doi:10.1016/j.trgeo.2016.06.002.

[24] Banerjee, S., Manna, B., & Shahu, J. T. (2024). Behaviour of Geocell Reinforcement in a Multi-Layered Flexible Pavement Under Repeated Loading. International Journal of Geosynthetics and Ground Engineering, 10(3), 1–17. doi:10.1007/s40891-024-00541-7.

[25] Önal, Y., Çalışıcı, M., Kayadelen, C., & Altay, G. (2023). A comparative experimental study of geocell and geogrid-reinforced highway base layers under repeated loads. Road Materials and Pavement Design, 24(12), 2877–2892. doi:10.1080/14680629.2023.2182126.

[26] George, A. M., Banerjee, A., Puppala, A. J., & Saladhi, M. (2021). Performance evaluation of geocell-reinforced reclaimed asphalt pavement (RAP) bases in flexible pavements. International Journal of Pavement Engineering, 22(2), 181–191. doi:10.1080/10298436.2019.1587437.

[27] Rayabharapu, V. K., & Saride, S. (2019). Geocell Reinforced Dense Sand Bases Overlying Weak Sand Sub-grades Under Repeated Loading. Ground Improvement Techniques and Geosynthetics. Lecture Notes in Civil Engineering, 14, Springer, Singapore. doi:10.1007/978-981-13-0559-7_32.

[28] Biswas, S., Hussain, M., & Singh, K. L. (2024). Behavior of Bamboo and Jute Geocell Overlaying Soft Subgrade under Repeated Wheel Loading. Journal of Materials in Civil Engineering, 36(2), 4023570. doi:10.1061/jmcee7.mteng-16528.

[29] Kolathayar, S., Aravind, C. A., & TG, S. (2021). Model Tests and Analytical Studies on Performance of Areca Leaf Cells as Cellular Confinement in Soil. Geomechanics and Geoengineering, 16(4), 237–248. doi:10.1080/17486025.2019.1664774.

[30] Kolathayar, S., Narasimhan, S., Kamaludeen, R., & Sitharam, T. G. (2020). Performance of Footing on Clay Bed Reinforced with Coir Cell Networks. International Journal of Geomechanics, 20(8), 4020106. doi:10.1061/(asce)gm.1943-5622.0001719.

[31] Hegde, A., & Sitharam, T. G. (2017). Experiment and 3D-numerical studies on soft clay bed reinforced with different types of cellular confinement systems. Transportation Geotechnics, 10, 73–84. doi:10.1016/j.trgeo.2017.01.001.

[32] Kolathayar, S., Sowmya, S., & Priyanka, E. (2020). Comparative Study for Performance of Soil Bed Reinforced with Jute and Sisal Geocells as Alternatives to HDPE Geocells. International Journal of Geosynthetics and Ground Engineering, 6(4), 53. doi:10.1007/s40891-020-00238-7.

[33] Al-Haddad, S. A., Fattah, M. Y., & Al-Ani, F. H. (2024). Protection of buried pipeline using geosynthetics–a review. Geomechanics and Geoengineering, 19(4), 503–518. doi:10.1080/17486025.2023.2288933.

[34] Raymond, M. S., & Leffler, W. L. (2006). Oil and gas production in nontechnical language. Choice Reviews Online, 43(08), 43-4690-43–4690. doi:10.5860/choice.43-4690.

[35] ASTM D5261-10. (2018). Test Method for Measuring Mass Per Unit Area of Geotextiles. ASTM International, Pennsylvania, United States. doi:10.1520/D5261-10R18.

[36] ASTM D5199-12. (2019). Standard Test Method for Measuring the Nominal Thickness of Geosynthetics. ASTM International, Pennsylvania, United States. doi:10.1520/D5199-12R19.

[37] ASTM D4632/D4632M-15a. (2023). Standard Test Method for Grab Breaking Load and Elongation of Geotextiles. ASTM International, Pennsylvania, United States. doi:10.1520/D4632_D4632M-15A.

[38] ASTM D4355-05. (2017). Standard Test Method for Deterioration of Geotextiles by Exposure to Light, Moisture and Heat in a Xenon Arc Type Apparatus. ASTM International, Pennsylvania, United States. doi:10.1520/D4355-05.

[39] ASTM D6241-14. (2022). Standard Test Method for Static Puncture Strength of Geotextiles and Geotextile-Related Products Using a 50-mm Probe. ASTM International, Pennsylvania, United States. doi:10.1520/D6241-14.

[40] ASTM D4751-21a. (2021). Standard Test Methods for Determining Apparent Opening Size of a Geotextile. ASTM International, Pennsylvania, United States. doi:10.1520/D4751-21A.

[41] ASTM D4991-99a. (2015). Standard Test Methods for Water Permeability of Geotextiles by Permittivity. ASTM International, Pennsylvania, United States. doi:10.1520/D4491-99AR14E01.

[42] ASTM D698-12(2021). (2021). Standard Test Methods for Laboratory Compaction Characteristics of Soil Using Standard Effort (12,400 ft-lbf/ft^3 (600 kN-m/m^3)). ASTM International, Pennsylvania, United States. doi:10.1520/D0698-12R21.

[43] State Corporation for Roads and Bridges. (2003). General Specification for Roads and Bridges (SORB/R9)—Hot Mix Asphaltic Concrete Pavement. Department of Planning and Studies, Ministry of Housing and Construction, Baghdad, Iraq.

[44] Kumar, V. V., Saride, S., & Zornberg, J. G. (2021). Mechanical response of full-scale geosynthetic-reinforced asphalt overlays subjected to repeated loads. Transportation Geotechnics, 30, 100617. doi:10.1016/j.trgeo.2021.100617.

[45] Tabatabaei Aghda, S. T., Ghanbari, A., & Tavakoli Mehrjardi, G. (2019). Evaluating the Applicability of Geocell-Reinforced Dredged Sand Using Plate and Wheel Load Testing. Transportation Infrastructure Geotechnology, 6(1), 21–38. doi:10.1007/s40515-018-00067-2.